Experimental/Theoretical Comparisons of the Turbulence in the Scrape-Off-Layers of Alcator C-Mod, DIII-D, AND NSTX*

J.L. Terry 1), S.J. Zweben 2), D.L. Rudakov 3), J.A. Boedo 3), K. Hallatschek 4), R.J. Maqueda 5), R.A. Moyer 3), B. Bai 1), C.J. Boswell 1), M. Greenwald 1), S. Krasheninnikov 3), B. LaBombard 1), D. Kopon 1), A.W. Leonard 6), M.A. Mahdavi 6), G.R. McKee 7), W.M. Nevins 8), B.N. Rogers 9), P.C Stangeby 10), D. Stotler 2), J.G. Watkins 11), W.P. West 6), D.G. Whyte 3), and X.Q. Xu 8)

1) MIT Plasma Science and Fusion Center, Cambridge, MA, USA
2) Princeton Plasma Physics Laboratory, Princeton, NJ, USA
3) University of California, San Diego, CA, USA
4) Max Planck Institute of Plasma Physics, Garching, Germany
5) Los Alamos National Laboratories, Los Alamos, NM, USA
6) General Atomics, San Diego, CA, USA
7) University of Wisconsin, Madison, WI, USA
8) Lawrence Livermore Laboratory, Livermore, CA, USA
9) Dartmouth University, Hanover, NH, USA
10) University of Toronto, Institute for Aerospace Studies, Toronto, Canada
11) Sandia National Laboratories, Albuquerque, NM, USA

e-mail contact of main author: terry@psfc.mit.edu

Abstract: The intermittent turbulent transport in the scrape-off-layers of Alcator C-Mod, DIII-D, and NSTX is studied experimentally. On DIII-D the fluctuations of both density and temperature have strongly non-Gaussian statistics, and events with amplitudes above 10 times the mean level are responsible for large fractions of the net particle and heat transport, indicating the importance of turbulence on the transport. In C-Mod and NSTX the turbulence is imaged with a very high density of spatial measurements. The 2-D structure and dynamics of emission from a localized gas puff are observed, and intermittent features (also sometimes called “blobs”) are typically seen. On DIII-D the turbulence is imaged using BES and similar intermittent features are seen. The dynamics of these intermittent features are discussed. The experimental observations are compared with numerical simulations of edge turbulence. The electromagnetic turbulence in a 3-D geometry is computed using non-linear plasma fluid equations. The wavenumber spectra in the poloidal dimension of the simulations are in reasonable agreement with those of the C-Mod experimental images once the response of the optical system is accounted for. The resistive ballooning mode is the dominant linear instability in the simulations.

1. Introducton

Evidence for intermittent convective radial transport in the Scrape-Off-Layers (SOL) of tokamaks has existed for a number of years [1]. Recently, studies aimed at investigating this phenomenon have yielded a much clearer picture of the SOL transport and its implications on divertor operation and possibly density limits [2]. Typically, detailed measurements of the turbulence have come from single or multi-point probe or optical measurements in the outboard SOL, and they generally show very strong evidence for intermittent, convective particle transport there. The physics of this intermittent transport is important since it may dominate the scrape-off-layer transport [2,3], carrying a large fraction of the net cross-field flux of particles and heat, and resulting in the flat or nearly flat density profiles observed in the far-SOLs of many tokamaks. The three magnetic confinement devices reported on here, Alcator C-Mod, DIII-D, and NSTX, exhibit many qualitatively similar features, e.g. large, intermittent events, high levels of SOL turbulence, and poloidal and radial motion of localized features (“blobs”). Yet the SOL plasmas in these devices are different in many respects, e.g. B,

	C-Mod	DIII-D	NSTX
n_e	$3x10^{19}$ m^{-3}	$5x10^{18}$ m^{-3}	$3x10^{18}$ m^{-3}
T_e	25 eV	25 eV	20 eV
L_p^{perp}	7 mm	20 mm	40 mm
ρ_s	0.18 mm	0.44 mm	3 mm
L_c	5 m	12 m	10 m
$L_o^{resist.\ ball.}$	~1 mm	~1 mm	~10 mm
L^{turb}_{pol}	~9 mm	~20 mm	~40 mm
$\tau_{auto\text{-}cor}$	20 μs	20 μs	40 μs
I_{sat}^{RMS}/I_{sat}	~40%	~40%	~40%
λ_{ei}/L_c	0.07	0.2	0.2
β	$3x10^{-5}$	$4x10^{-5}$	$8x10^{-4}$

TABLE 1. Comparison of quantities characterizing SOLs of specific L-mode plasmas in the three devices, evaluated at the outboard midplane, ~1 density e-folding length outside the separatrix.

λ_{ei}/L_c, ρ_s, gradient scale length. A SOL comparison for moderate to high density L-mode discharges in each device is shown in Table 1. (L_p^{perp} is the pressure scale length; L_c is the parallel connection length, $L_o = L_c [n_e e^2 \eta_{\parallel} \rho_s/(R m_i \omega_{ci})]^{0.5} (2R/L_p)^{0.25}$ is the characteristic size scale for the (linear) resistive ballooning mode [4]; L^{turb}_{pol} is the measured poloidal correlation length of the turbulence; $\tau_{auto\text{-}cor}$ is the FWHM of the fluctuation autocorrelation function at a stationary point; λ_{ei} is the electron-ion mean free path.) It is the purpose of this paper to report and compare observations from these devices, and to compare some of the experimental results with simulations of the edge plasma in hopes of understanding the underlying turbulence.

2. Intermittent Fluctuation-Driven Transport Fluxes

In the outboard SOL of DIII-D, the fluctuating components of the electron density, electron temperature and poloidal electric field are simultaneously measured using a reciprocating Langmuir probe array. From these measurements the cross-field fluctuation-driven particle and heat fluxes are derived. The fluctuations of both density and temperature have strongly non-Gaussian statistics characterized by positive skewness and kurtosis. Conditional averaging was used to characterize typical events in fluctuations and fluxes. The intermittent large-density events correlate with the occurrence of spikes in the poloidal electric field and result in intermittent transport events carrying both particles and heat. The intermittence has qualitatively similar character in L-mode and ELM-free H-mode. However, the absolute transport rates due to intermittence are much higher in L-mode. Figure 1 shows the contribution of intermittent events to net particle and heat fluxes. Each point represents the fraction of the total flux carried by all events with relative amplitudes greater than the x-axis

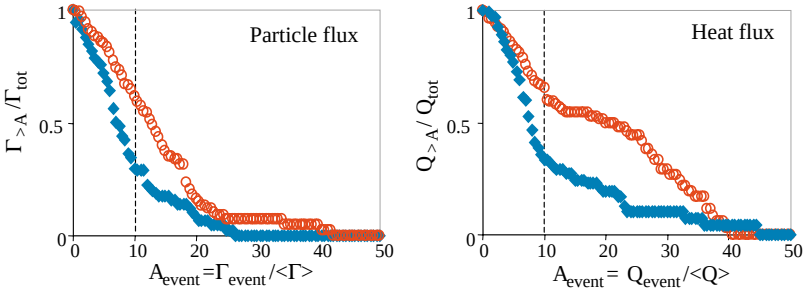

Fig. 1. Fraction of the total particle and heat flux in DIII-D carried by transport events with relative amplitude A_{event} greater than the corresponding x-axis value. (A_{event} is normalized to the mean flux.) Open circles are for L-mode; solid diamonds are for ELM-free H-mode. The measurements are made ~15 mm outside the separatrix.

value. Events with amplitudes above 10 times the mean level are responsible for ~60% of the net particle and heat transport in L-mode and for ~30% of the net transport in H-mode. These and other similar measurements on other devices demonstrate the importance of understanding the turbulence that underlies this transport.

3. "Imaging" the turbulence

The turbulence that is presumably responsible for the transport documented above has been investigated on all three devices. In Alcator C-Mod and in NSTX the edge/SOL turbulence is imaged with a very high density of high resolution spatial measurements [5,6] and studied with probes. In DIII-D the density fluctuations are imaged directly with moderate spatial resolution and coverage using BES [7] and studied with probes. As seen in Table 1, the size scales of the turbulent features, L^{turb}, as well as scales, L_p, ρ_s, and L_o vary by almost an order of magnitude. The imaging in C-Mod and NSTX is accomplished by viewing (parallel to the local field) line emission from a localized gas puff [5,6]. The detailed 2-D structure and dynamics of the emission are measured using gated and high frame-rate (up to 1 MHz) cameras. Complex emission patterns are typically observed. Examples from NSTX and C-Mod are shown in Figure 2. The larger size scale in the NSTX images is obvious. Often the localized, intermittent features, as well as "wave-like" poloidal structures are observed. On C-Mod the larger features move at speeds up to ~0.5 km/s. The atomic physics that converts the density and temperature fluctuations into fluctuations in emission complicates the quantitative interpretation and has been studied in [5,8]. The details will not be repeated here except to say that the atomic physics "windows" an observable region, limited on the hot side by ionization and on the wall side by lack of excitation. Nonetheless, within this "window" the emission responds to the fluctuations approximately as $n_e^{\alpha}T_e^{\beta}$, with α, β between 0.3 and 1.4 [8]. Wavenumber spectra in the poloidal and radial planes are measured and used for quantitative comparison with the theoretical simulations (Section 4). In C-Mod there is no clear difference in structure size between L- and H-mode plasmas [5]. In NSTX differences are seen since the emission "window" includes the H-mode pedestal. As evidenced in Figs 2b) and 3a), the turbulent features often appear to be formed near the LCFS [9] and propagate predominately outward and poloidally at about $\mathbf{E_r}$ x $\mathbf{B}$ velocity. Fig. 2b) shows a special case near the density

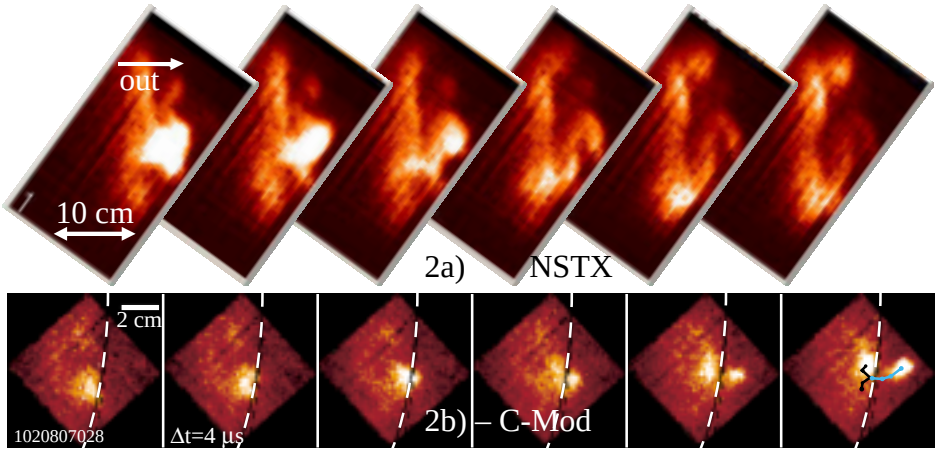

Fig. 2. Sequences of experimental images from NSTX and C-Mod, showing space and time evolution of turbulence at the outboard SOL. In 2b) the white-black line is the LCFS. In the last frame the lines track the motion of each blob.

limit ($n/n_{GW}\approx0.7$) in C-Mod, where a blob is seen on *closed* flux surfaces. As the blob crosses the LCFS, it splits, and the portion on open field lines moves out radially. Fig. 3(a) shows two frames of DIII-D BES data (2-D density plots). It is clear that the object is moving poloidally and radially with speeds that can be easily estimated to be $V_\theta\approx5$ km/s and $V_r\approx1.5$ km/s. The propagation velocities can be estimated independently using probe data, such as shown in Fig. 3b). The traces shown result from conditional averaging (over ~ 20 events) at about 0.5 cm outside the LCFS. A poloidal velocity of ≈4.5 km/s was estimated from the time delay between two floating potentials (top traces) measured by two poloidally separated probe tips. A radial velocity of ≈2.5 km/s was estimated from the poloidal field inside the blob (bottom trace) assuming the propagation is due to $\mathbf{E_\theta}$ x **B** drift. Both velocities decrease with the distance from the LCFS in the SOL. The transverse object size, 1-3 cm near the LCFS, remains relatively unchanged between L and H-modes, although the amplitude decreases [10]. As the objects move towards the wall, they shrink in size and decay in amplitude [9].

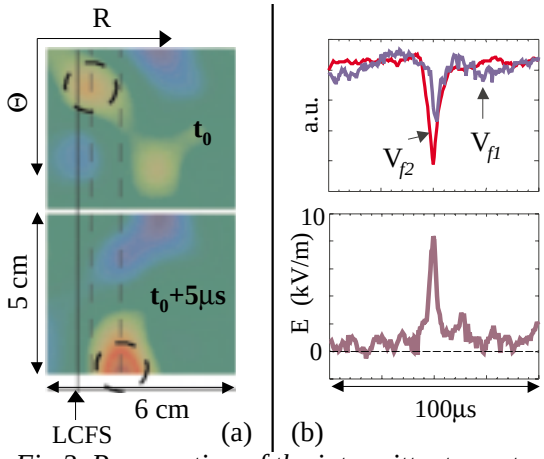

Fig 3. Propagation of the intermittent events in DIII-D: (a) data from BES - the radial motion of a positive density feature of roughly 2 x 2 cm extent, marked by a dashed circle, is indicated by vertical dashed lines: (b) data from midplane probe array

4. Comparisons with Simulations.

In addition to the improvements in experimentally diagnosing the edge turbulence, recent advances in the numerical modeling of edge turbulence now allow detailed comparison with the experimental observations. In particular, we are able to compare directly the characteristics of the 2-D radial vs. poloidal turbulence calculated from 3-D non-linear drift-ballooning codes [4,11] with those of the experimental images. A simulation using time-averaged profiles measured in the outboard SOL of C-Mod has been done. The simulation solves the Braginskii fluid equations for electrons and ions in a 3-D geometry (note $\lambda_{ei}/L_c<0.1$). It includes diamagnetic, magnetic shear, and toroidal curvature effects, and mimics the effect of open field lines ending on outboard limiters located 1 and 2 m away. A separatrix and X-pt are not included. The inclusion of open lines ending at the divertor does not influence the results and indicates that the SOL turbulence field is not driven primarily by flute-like instabilities. Inclusion of open field lines ending on the outboard limiters does alter the shape of the simulation's k-spectrum, indicating its importance in setting boundary conditions in the simulation. The comparison of the simulation results with the measured edge turbulence in C-Mod shows that the average size-scales, fluctuation amplitudes, and particle fluxes agree to within about a factor of two. A more rigorous test is to compare the k_{pol} spectral shapes, as is done in Figure 4, where an experimental NSTX k-spectrum is also shown. The simulation's density fluctuation spectrum has relatively more structure between k=5 and 30 cm^{-1}. However,

including the effects of 1) the atomic physics "windowing", 2) a 2 μs time-average, and 3) most importantly the measured spatial response of the experimental optical system (Δk_{HWHM}~12 cm^{-1}) results in the apparent suppression of the smaller-scale features and in the good match shown in Figure 4. Although the developed state of the turbulence is highly non-linear, the dominant linear instability in the simulation is the resistive ballooning mode. Its scale size L_o is ~1 mm in C-Mod, ~10 mm in NSTX, and ~1 mm in DIII-D, showing a scaling roughly consistent with the machines' turbulence size scales.

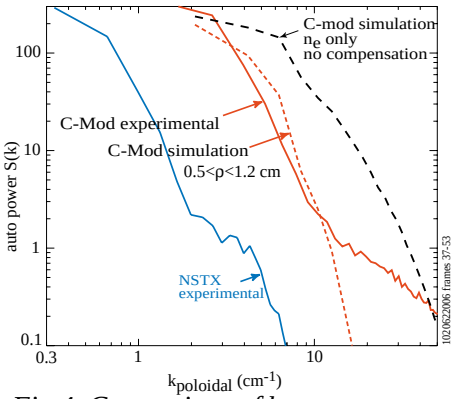

Fig 4. Comparison of k_{pol} spectrum from C-Mod with simulation and with an experimental spectrum from NSTX. The short dashed simulation spectrum has experimental time and spatial resolutions folded in.

An initial comparison with the C-Mod observations has also been done using another 3D non-local electromagnetic turbulence simulation code, BOUT [11], which models boundary-plasma turbulence with a realistic separatix and X-pt geometry. It also shows a good match with the experimental k-spectrum, although the time-averaged input profiles were somewhat different from those measured. The dominant linear instability is the resistive X-pt mode, which is resistive ballooning in the proper X-pt geometry. The ballooning character of the turbulence in the simulations is also manifested in the predictions of much reduced turbulence and transport at the inboard side of the plasma. This is seen in C-Mod where the normalized intensity fluctuation, as observed by a radial array of views just in front of an *inboard* midplane gas puff, is approximately a factor of ten smaller than that measured *on the same flux surface* at the outboard midplane. Inboard and outboard probe measurements of I_{sat}^{RMS}/I_{sat} give similar results.

All three experiments show radial propagation of the turbulent structures, with speeds up to ~1.5 km/s. It has been proposed [12] that radial blob propagation on open field lines is driven by ExB forces resulting from polarization within the blob's flux tube. Many of these observations are consistent with this picture, e.g. the DIII-D measurements and the C-Mod movie of Figure 2b), where the radial speed changes as the blob "splits" at the LCFS.

[1] M. ENDLER *et al.*, Nucl. Fus. **35** (1995) 1307; also B. K. JOSEPH *et al.*, Phys. Plasmas **4** (1997) 4292.
[2] B. LABOMBARD *et al.*, Phys. Plasmas **8** (2001) 2107; M. GREENWALD, Plasma Phys Cont Fusion **44** (2002) R27
[3] Y. SARAZIN AND PH. GHENDRIH, Phys. Plasmas **5** (1998) 4214; also A. HUBER *et al.*, J. Nucl. Mat. **266-269** (1999) 546; also B.A. CARRERAS *et al.*, Phys. Plasmas **8** (2001) 3702; also J.A. BOEDO *et al.*, Phys. Plasmas **8** (2001) 4826.
[4] B.N. ROGERS *et al.*, PRL **81** (1998) 4396.
[5] S.J. ZWEBEN *et al.*, Phys. Plasmas **9** (2002) 1981.
[6] R.J. MAQUEDA *et al.*, to be published in Rev. Sci. Instrum. (2002); also S.J. ZWEBEN *et al.*, EPS (2002)
[7] G.R.MCKEE *et al.*, Rev.Sci.Instrum. 70 (1999) 913.
[8] D. STOTLER *et al*, to be published in J. Nucl. Mater. (2002)
[9] J.A. BOEDO *et al.*, to be published in in J. Nucl. Mater. (2002)
[10] D.L. RUDAKOV *et al.*, Plasma Phys. Cont. Fusion **44** (2002) 717.
[11] X.Q. XU *et al.*, Phys. Plasmas **7** (2000) 1951; also X.Q. XU *et al.*, New Journal of Physics **4** (2002) 53.
[12] S.I. KRASHENINNIKOV, Phys. Lett. A **283** (2001) 368; also D. D'IPPOLITO *et al.*, Phys. Plasmas **9** (2002) 222.
*Work supported by USDOE Cooperative Agreement DE-FC02-99ER54512, Contracts DE-AC02-76CHO3073, DE-AC03-99ER54463, W-7405-ENG-48 and DE-AC04-94AL85000, and Grants DE-FG03-95ER54294, and DE-FG03-96ER54373.